JOURNAL OF RAMAN SPECTROSCOPY
J. Raman Spectrosc. 2004; **35**: 947–955
Published online 16 September 2004 in Wiley InterScience (www.interscience.wiley.com). DOI: 10.1002/jrs.1239

JRS

Comparative vibrational analysis of thyronine hormones using infrared and Raman spectroscopy and density functional theory calculations

Rosa M. S. Álvarez,[1] Ricardo N. Farías[1] and Peter Hildebrandt[2]*

[1] Departamento de Bioquímica de la Nutrición, Instituto Superior de Investigaciones Biológicas (INSIBIO), CONICET and Universidad Nacional de Tucumán, Chacabuco 461, (4000) San Miguel de Tucumán, Tucumán, Argentina.
[2] Technische Universität Berlin, Institut für Chemie, Max-Volmer-Laboratorium, Sekr. PC 14, Strasse des 17. Juni 135, D-10623 Berlin, Germany

Received 22 May 2004; Accepted 3 July 2004

The molecular structures of L-thyroxine (T4), 3,5,3′-triiodo-L-thyronine (T3) and 3,5-diiodo-L-thyronine (T2) were investigated by means of vibrational spectroscopy and density functional theory calculations using the B3LYP hybrid functional and the SDD effective core potential basis set, suitable for heavy atoms. The experimental data were obtained from FT-IR and Raman spectra of the thyroid hormones in the crystalline state. The combined experimental and theoretical approach allows a consistent assignment for most of the fundamental modes in the range between 100 and 1650 cm^{-1}. It was found that, in general, the modes are largely localized in the individual rings and in the linkage connecting both rings. Hence it was possible to identify bands that are dominated by the internal coordinates of the ether bridge and the C–I stretchings. These bands are considered to be sensitive spectral markers for monitoring conformational changes of the hormones after insertion into phospholipid bilayers. Copyright © 2004 John Wiley & Sons, Ltd.

KEYWORDS: vibrational analysis; density functional theory; Fermi resonance; hormones; membrane binding

INTRODUCTION

Thyroid hormones must be taken up by target cells to act at the genomic level through binding to nuclear thyroid hormone receptors. Extensive studies have been carried out on the mechanisms by which thyroid hormones, bound to the thyroid hormone receptors, regulate transcription. However, as yet little is known about the critical upstream step, i.e. how thyroid hormones enter the cell. Growing evidence indicates that saturable transport mechanisms mediate the greater part of thyroid hormone movement across the plasma membrane and play important roles in the regulation of thyroid hormone bioavailability.[1] To gain insight into the non-genomic mechanisms of the thyroid hormones, we have previously studied the interactions and transmembrane diffusion of theses hormones with the liposomes membrane from dimyristoyl- and dipalmitoylphosphatidylcholine in the liquid-crystalline and gel phase and egg yolk phosphatidylcholine/cholesterol in the liquid-ordered phase.[2–4] The assumption that thyroid hormones easily penetrate plasma membranes was strengthened by Hillier[5] using liposomes prepared from egg-yolk phosphatidylcholine. However, there is evidence that thyroid hormones are normal constituents of the biological membrane in vertebrates and physiological effects of these hormones occur at membranes.[6] The hormones are strongly associated with membranes in tissues and normally decrease the mobility of these membranes, influencing their lipid compositions. It is suggested that both effects on the physical state of the membrane and the changes in membrane composition result in several other thyroid hormone effects.[6] It has been reported also that thyroid hormones alter the membrane dipolar organization.[7,8]

Recently, we have presented a Raman spectroscopy study of the conformational changes of thyroxine induced by interactions with phospholipids. The conclusions were derived from differences between the spectra of L-thyroxine (T4) in the pure solid state and the spectra of the membrane complex.[9] For understanding the specific hormone–membrane interactions in more detail, a sound vibrational analysis of the various thyronines is required, which was the goal of the present study.

We report a comparative analysis of the infrared and Raman spectra of 3,5,3′-triiodo-L-thyronine (T3), 3,5-diiodo-L-thyronine (T2) and T4 in the crystalline state.

*Correspondence to: Peter Hildebrandt, Technische Universität Berlin, Institut für Chemie, Max-Volmer-Laboratorium, Sekr. PC 14, Strasse des 17. Juni 135, D-10623 Berlin, Germany.
E-mail: hildebrandt@chem.tu-berlin.de

JRS

The experimental studies were complemented by quantum chemical calculations (B3LYP/SDD). Optimized geometries were compared with the available crystal structure data for T3 and T4.[10] The calculated spectra served as a basis for the assignments of the experimental Raman and infrared bands.

EXPERIMENTAL

T4, T3 and T2 were purchased from Sigma Chemical (St. Louis, MO, USA) and used without further purification.

Infrared spectra of the three iodothyronines in KBr pellets were measured between 400 and 4000 cm^{-1} with an FT-IR spectrometer (Perkin-Elmer 1600, 4 cm^{-1} resolution). Raman spectra between 100 and 4000 cm^{-1} were recorded with a Bio-Rad FT Raman spectrometer (4 cm^{-1} resolution, 1064 nm excitation) using a 180° backscattering geometry.[11] The solid pure hormones were deposited in quartz tubes of 0.25 cm inner diameter. In order to achieve a sufficient signal-to-noise ratio, 8192 scans were accumulated for each substance, corresponding to a total accumulation time of ~5 h in each case.

Quantum chemical calculations were carried out with the Gaussian 98 program package[12] on a personal computer for geometry optimization and calculation of the vibrational spectra. Density functional theory (DFT) calculations were performed by using the B3LYP hybrid functional and the SDD effective core potential basis set suitable for heavy atoms. It was not possible to use higher levels of theory owing to the presence of iodine atoms in the systems. However, comparative calculations for small organic molecules demonstrated that the SDD basis provides results of nearly the same quality as the 6–31G* basis set.

The calculations were performed for molecules in vacuum such that environmental effects are not considered. Hence the energy optimum was calculated to be the neutral form whereas in the solid state or in neutral aqueous solution the zwitterionic form exists.

Optimized structures of various conformers were obtained by scanning the dihedral angles of the rings with respect to the ether bridge, represented by ϕ and ϕ', of the alanyl side-chain with respect to the α ring (ψ) and of the amino acid group (χ) (Fig. 1).

RESULTS AND DISCUSSION

Structures of the thyronines

Geometry optimizations were carried out for T2, T3 and T4. Specific attention was paid to the orientation of the aromatic rings with respect to each other. This structural parameter can be described in terms of the angle formed by the normal to the plane through each ring and the normal to the plane through the three atoms of the ether linkage. Mutual orientations of the phenyl rings were performed by scanning ϕ and ϕ' at 30° intervals from 0° to 180°. In the same way, the dihedral angles ψ and χ were optimized.

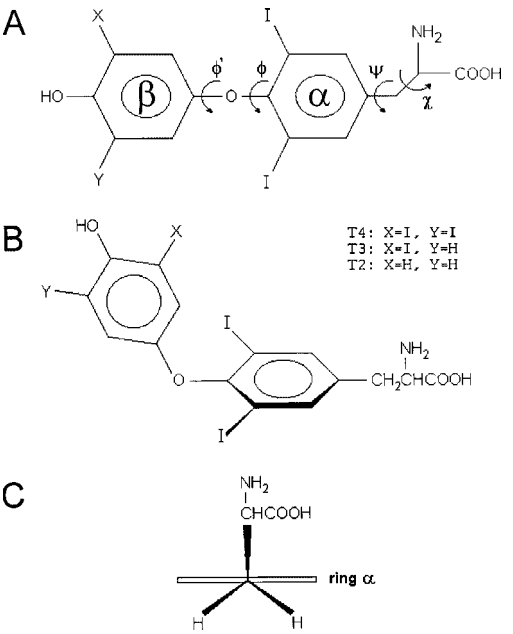

Figure 1. (A) Definition of torsion angles of thyroid hormones; (B) conformation of thyroid hormones derived form the geometry optimization; (C) schematic presentation of the amino acid group relative to the plane of ring α.

With respect to the mutual orientation of the aromatic rings, the results show slight deviations of the α and β rings from the perpendicular and parallel orientation with respect to the ether bridge plane such that steric hindrance of the phenolic ring β and the iodine atoms on the α ring are minimized (Fig. 1).

In general, these structures agree with previous results obtained for the conformations of thyroxin and its analogues, in which the two aromatic rings adopt an approximately perpendicular orientation.[13–15]

Very similar overall conformations are predicted for T2 and T3. For T3, the orientations of the rings α and β determined from the crystal structure are well reproduced. Only for T4 are significant deviations noted on comparing the calculated and crystal structures.[10] This discrepancy may not necessarily reflect a deficiency in the calculations since the experimental data are associated with high standard deviations, which, on the one hand, have been attributed to a low quality of the crystals. On the other hand, the dominant contributions of the x-ray scattering from the iodine atoms leads to lower precision in localizing the lighter atoms carbon, oxygen and nitrogen.[10] Selected structural parameters are given in Table 1.

The dihedral angle ψ describes the orientation of the alanyl side-chain with respect to the α ring. The calculated values for T2, T3 and T4 are 118.4, 103.6 and 100.7°, respectively, which imply that the C_{sp^3}—C_{sp^3} bond is roughly perpendicular to the aromatic ring. These results agree with the x-ray structure of T4 (Fig. 1).[16]

Table 1. Calculated and experimental structural parameters for T4 and T3

	T4		T3		T2
Internal coordinate[a]	B3LYP/SDD	Experimental[b]	B3LYP/SDD	Experimental[b]	B3LYP/SDD
I—C	2.14	2.11	2.15	2.11	2.14
Phenyl C—C	1.41	1.40	1.41	1.41	1.41
Phenyl C—O	1.40	1.41	1.40	1.34	1.40
Phenyl CCC angle	120.1	119.4	120.3	119.1	120.3
COC angle	120.9	118 ± 3	121.0	121 ± 3	121.0
$\phi\alpha$-Ring–ether plane	92.3	101	94.6	90	93.3
$\phi\beta$-Ring–ether plane	0.6	−34	−1.3	−13	−1.9

[a] Bond lengths and angles are given in Å and degrees, respectively.
[b] Experimental data are taken from Ref. 10.

Finally, the lowest energy for the three iodothyronines were reached with the non-ionic amino acid entity oriented in such a way that the COOH and NH_2 groups are *anti* and *gauche* to the α ring, respectively. SVWN/6–31G* calculations for the non-zwitterionic tyrosine phenoxyl radical indicate that in the lowest energy conformation both the COOH and NH_2 groups are *gauche* with respect to the phenoxyl ring,[17] in agreement with the neutron diffraction structure of zwitterionic L-tyrosine.[18] The *anti* conformation for the COOH group is calculated to be 8.08 kJ mol^{-1} higher in energy.[17]

Attempts to obtain the same orientation for the amino acid groups of T2, T3 and T4 were not successful. For T2 the B3LYP/SDD calculations with the COOH and NH_2 groups *gauche* to the α ring yield an energy that is higher by 7.61 kJ mol^{-1} than the structure with the COOH group in an *anti* conformation. The optimization of such a configuration of T3 failed, whereas a stable structure was reached for T4 with an energy that is higher by 12.6 kJ mol^{-1}.

Calculated vibrational spectra

The vibrational spectra calculated for the various conformers do not exhibit notable differences such that the assignment of the experimental Raman and IR spectra is based on the spectra calculated for lowest energy conformations.

Calculated forces constants and thus calculated wavenumbers are generally overestimated owing to the errors associated with the harmonic approximation and the insufficient consideration of electron correlation effects. It has been shown previously that scaling the force field can efficiently compensate these errors.[19,20] In this way, accuracy in the wavenumber calculation of ca 10 cm^{-1} can be achieved. At the B3LYP/6–31G* level, the scaling factors that refer to different internal coordinates are very similar. Therefore, we simplified the procedure by adopting a uniform factor equal to 0.9743 to scale the wavenumbers directly. Determination of this factor was based on the highest wavenumber ring modes $\alpha(1)$ and $\beta(1)$ that give rise to the strongest Raman bands between 1570 and 1600 cm^{-1}.[21] The factor was chosen such that the best agreement was achieved between the calculated and the experimental wavenumbers for the three iodothyronines. This simplified scaling procedure is associated with an average error of the wavenumbers prediction that is estimated to be higher by a factor of 2 than in the case of force field scaling. Nevertheless, this reduced accuracy is considered to be sufficient for a consistent assignment of most of the observed bands. Moreover, additional assignment criteria are provided by the calculated Raman and IR intensities, which were classified semiquantitatively in terms of very strong (vs), strong (s) medium (m), weak (w) and very weak (vw) bands.

Table 2 lists the scaled calculated wavenumbers and intensities and the experimental IR and Raman wavenumbers and intensities along with a tentative assignment for most of the fundamentals.

Vibrational assignment

For the three molecules, the 99 normal modes of vibration are all active in the infrared and Raman spectra. All calculated modes that originate from the COOH and NH_2 groups were not considered for the band assignments, since in the solid state thyroid hormones adopt the zwitterionic form. In the experimental IR spectrum, there are strong and complex signals around 1600 cm^{-1} which originate from the vibrations of the $(NH_3)^+$ and $(CO_2)^-$ groups whereas no C=O stretching bands of the protonated carboxyl groups could be detected. Hence it is concluded that the amino acids of T2, T3 and T4 exist in a zwitterionic structure. In contrast to the IR bands, the Raman bands of the zwitterionic forms exhibit only very weak intensity.

The following assignments will be restricted to those spectral regions in which differences have been noted upon complex formation of the hormones with phospholipids[9] (R. M. S. Álvarez, unpublished results). In general, the modes originating from ring α do not differ very strongly between T2, T3 and T4 whereas for the ring β modes substantial differences are noted owing to the different substitution patterns.

The aromatic ring vibrations give rise to four medium and strong Raman bands between 1530 and 1620 cm^{-1} (Fig. 2).

Table 2. Calculated and experimental wavenumbers (cm^{-1}), relative intensities and tentative assignments for T2, T3 and T4

T2[a]			T3[a]			T4[a]			
B3LYP/SDD	IR	Raman	B3LYP/SDD	IR	Raman	B3LYP/SDD	IR	Raman	Assignment[b,c]
1622vw,s		1611m	1610w,s		1605sh	1591m,vs		1579s	$\beta(1)$; $\beta(1)$; $\beta(1)+\alpha(1)$
1607vw,w		1601m	1582w,w		1593sh	1576w,vs		1579s	$\beta(2)$; $\beta(2)+\alpha(1)$; $\beta(1)-\alpha(1)$
1578w,vs		1580s	1577w,vs		1574s	1560m,s		1566m	$\alpha(1)$; $\alpha(1)-\beta(2)$; $\beta(2)$
1535m,m		1541m	1537m,m		1534m	1537m,m	1539m	1537m	$\alpha(2)$
1494s,w	1505s		1469vs,w	1461m	1450w	1440s,w	ovl		$\beta(3)$
1482w,w		1505w	1482w,w	1477w	1450w	1482w,w			$\delta_{sym}CH_2$
1431w,w	1448sh	1448w	1425s,w	1436s	1433sh	1423s,w	1433s	1439m	$\beta(4)+\alpha(3)$; $\alpha(3)$; $\alpha(3)$
1423s,w	1437s		1404vw,m		1395w	1393m,w	ovl	1381w	$\alpha(3)-\beta(4)$; $\beta(4)$; $\beta(4)$;
1385m,w	1392m	1396w	1385m,w	1395sh		1384m,w		1381w	$\alpha(4)$
1351w,w			1343w,m	1350w	1333w	1328m,m	1319w	1315w	$\beta(5)$
1350m,m	1344m	1349m	1359w,w	1350w	1333w	1359vw,w	1356w	1356w	$\delta C_{sp^3}-H$
1336vw,m		1325sh	1339m,s	1328w	1333w	1338s,s	1330w	1328w	CH_2 wag
1308w,w			1292w,w						$\beta(6)$
1301w,m		1269w	1299w,s		1282m	1299w,s		1291m	$\alpha(5)$
						1275s,m	1289w	1291m	$\delta_{i.p.}OH$
1269w,m		1269w	1270vw,m	1267sh	1267m	1270vw,m		1267w	CH_2 twist
1249m,w	overlap.	overlap.	1250m,w	1254s	1246m	1232vw,s	1239s	1239m	$\nu C-O(\alpha)/C-OH_{o.o.ph.}$
1228s,s	1233s	1233s	1225s,s	1233sh	1236m	1223s,s	1229sh	1229sh	$\nu C-O(\alpha)/C-OH_{i.ph.}$
1211w,w	1211sh	1209w	1211w,w	ovl	ovl	1210w,w			νC(sp3)–C(sp2)
1204w,vw			1204vw,w			1205vw,w			$\alpha(7)$
1176m,w									$\alpha(8)$
1156m,m	1187s	1190w	1166s,w	1182s	1182w	1168w,w	1183m	1177w	$\nu C\beta-O$
1136s,m	1162m	1154s	1151m,w	1136w	1135w	1119s,w	1155w		$\delta OH_{i.p.}$
1125w,w			1104vw,w			1103vw,w			$\nu C_{sp^3}-C_{sp^3}$
1096m,w	1097m		1113w,w						$\beta(7)$
1085w,m	1055w	1055vs	1094w,m	1052m	1058vs	1092w,m	1050w	1053s	$\nu C-N$
1038w,s	1029w	1029w	1038w,s	1027m	1027m	1038w,s	1048sh	1038s	$\alpha(9)$
1001w,vw	1009w		1012w,m			1028vw,s		1038s	$\beta(9)$
976vw,vw			972vw,vw			910w,w			$\beta(10a)$; $\beta(10b)$; $\beta(10c)$
936vw,vw			878w,w			892w,w			$\beta(11a)$; $\beta(11b)$; $\beta(11c)$
921w,w			920vw,w			923vw,w			$\alpha(10c)$
918w,w			916vw,w			918vw,w			$\alpha(11c)$
880m,w	877m	894w	882m,w	875w	889w	881m,w	882m	891w	$\alpha(12)$
846m,vw									$\beta(13)$
833w,m	855sh	850m	853w,m	825m		864vw,m	850m	850m	$\beta(12)$
811w,vw			837w,vw		834s, ovl				$\beta(14a)$; $\beta(14b)$
801m,s	814s	814s	801m,s	811m		801m,s	828m	828m	α/β ring deformation
784m,m	772m	717w	772s,w	778m	787w	770s,w	779w	782w	NH_3^+ wag
763w,w			765m,w	778m	787w	765m,w		782w	$\alpha(15)$
708vw,w			706vw,w			726w,w	722m	722w	$\beta(15)$
696m,w	710m	701w	701w,w	705m	701w	704w,w	710m	707w	δOCO
692m,w	704m		692m,w	705m		694m,w	700m	700w	$\alpha(16)$; $\alpha(16)$; $\alpha(16)+\beta(16)$
632vw,m	642w	642m	644vw,w	656w	660m	693m,w	700m	700w	β (16); β (16); $\beta(16)-\alpha(16)$
514vw,w			514vw,w			514vw,w			$\alpha(17)$
512w,vw			556vw,w			577vw,vw			β (18)
504vw,w			447w,w						$\beta(17)$
420vw,vw			445vw,vw			492vw,w	430vw		$\tau\beta$
399vw,w		380m							$\delta_{o.o.p.}C\alpha$-residue
392vw,w		380m	360s,w						$\delta_{i.p.}$C–OH (phenol)

Table 2. (*Continued*)

T2[a]			T3[a]			T4[a]			
B3LYP/SDD	IR	Raman	B3LYP/SDD	IR	Raman	B3LYP/SDD	IR	Raman	Assignment[b,c]
368vw,w		366w	368vw,w		376w	369vw,w		365sh	$\delta_{i.p.}C\alpha$-residue
347vw,w		359w	351vw,w		342s	357vw,w		340w	$\beta(19)$
301s,w		305w	360s,w		367w	341s,w		388m	$\delta_{o.o.p.}$OH (phenol)
						246vw,w		245sh	$\nu_{asym}C-I\beta$
230vw,w		246w	236w,w		245s	237vw,vw		ovl	$\nu_{asym}C-I\alpha$
						225vw,w		220vs	$\nu_{sym}C-I\beta$
			223vw,w		ovl				$\nu C-I\beta$
			200vw,w						$\delta C-I\beta$
183vw,w		184vs	190vw,w		187vs	214vw,w		190vs	$\nu_{sym}C-I\alpha$
						180vw,vw			$\delta_{o.o.p.asym}C-I\beta$
177vw,w		163sh	170vw,w		164sh	171vw,w			$\delta_{o.o.p.asym}C-I\alpha$
						167vw,w		152s	$\delta_{o.o.p.sym}C-I\alpha$
						153vw,w		152s	$\delta_{i.p.asym}C-I\alpha$
			144vw,w		156sh				$\delta_{o.o.p.}C-I\beta$

[a] Band intensities are classified by weak (w), very weak (vw), medium (m), strong (s) and very strong (vs). For calculated band intensities, the first and the second symbols refer to IR and Raman intensity, respectively. Shoulder and overlapping bands are denoted by 'sh' and 'ovl', respectively.

[b] The patterns of the ring modes $\alpha(k)$ and $\beta(k)$ for $k = 1–19$ are illustrated in Fig. 3.

[c] δ, deformation; ν, stretching; τ, torsion; sym, symmetric; asym, antisymmetric; wag, wagging; twist, twisting; i.p., in-plane; o.o.p., out-of-plane; i.ph., in-phase; o.o.ph., out-of-phase.

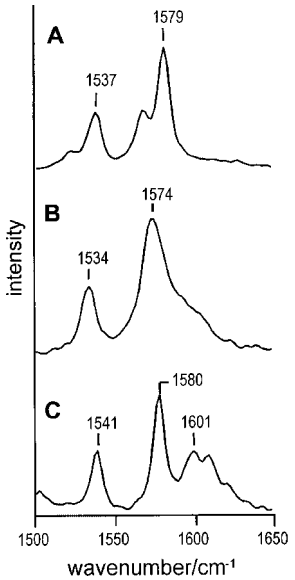

Figure 2. Raman spectra of (A) T4, (B) T3 and (C) T2 in the region between 1500 and 1650 cm^{-1}.

The experimental bands reveal good agreement with the calculated data with respect to both the wavenumbers and the intensities. The mode patterns can be described by in-phase and out-of-phase combinations of the aromatic ring modes (1) and (2) of both rings (Fig. 3), which are analogous to the tyrosine modes ν_{8a} and ν_{8b}, respectively.[21] Specifically, we note strong coupling of the modes $\beta(2)$ and $\alpha(1)$ for T3, whereas in T4 coupling of the modes $\beta(1)$ and $\alpha(1)$ gives rise to two modes that may contribute to the strong band at 1579 cm^{-1}.

Modes including the C–O stretching coordinate of the phenol group and the ether bridge are expected in the region between 1100 and 1300 cm^{-1} (Fig. 4). These modes can be considered as sensitive indicators for hormone binding to phospholipid bilayer which leads to the insertion of the phenyl group into hydrophobic lipid core and affects the geometry of the ether bridge.[22]

The calculations show that, in contrast to the C–O(β) stretching, the C–O(α) stretching is coupled with a variety of different internal coordinates including the C–OH stretchings of ring β. Thus, for each of the compounds two modes can be identified that can be described as in-phase and out-of-phase C–O(α)/C–OH stretchings. For T2, the in-phase C–O(α)/C–OH stretching mode is calculated at 1228 cm^{-1} and assigned to the strong experimental band centred at 1233 cm^{-1} in both the IR and the Raman spectra. This band overlaps with a weaker band at 1249 cm^{-1} that is attributed to the out-of-phase vibration.

The IR spectrum of T3 shows a broad band centred at 1254 cm^{-1} with shoulders on both sides of the peak, which is much better resolved in the Raman spectrum. The in-phase C–O(α)/C–OH vibration, calculated at 1225 cm^{-1}, is attributed to the 1236 cm^{-1} band whereas the 1246 cm^{-1} band is assigned to the out-of-phase C–O(α)/C–OH mode, in good agreement with the calculated wavenumber value of 1250 cm^{-1}.

JRS

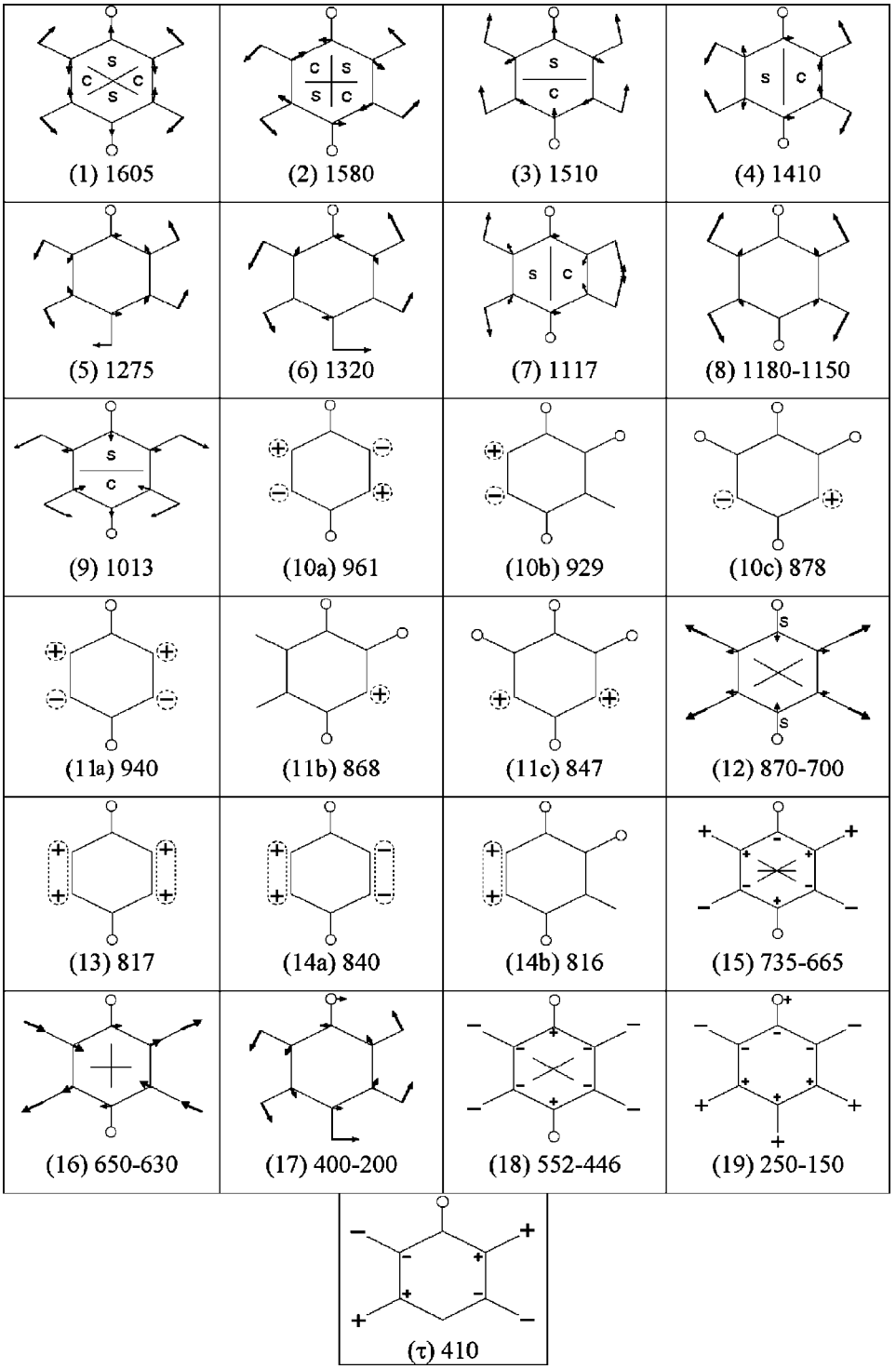

Figure 3. Representation of the mode patterns for selected calculated modes. The numbering refers to the ring modes $\alpha(k)$ and $\beta(k)$ for $k = 1–19$ as listed in Table 2.

In thyroxine, both aromatic rings are identically substituted at the *ortho*-positions. Correspondingly, the calculated wavenumbers for the in-phase and out-of-phase C–O(α)/C–OH modes are more closely spaced than those of T2 and T3. The experimental spectra show a sharp band at 1239 cm^{-1} with a well-defined shoulder of medium intensity at 1229 cm^{-1}. The assignment proposed in Table 2 follows the calculated wavenumbers. However, a reversed assignment is also possible on the basis of the predicted and observed intensities. The C–O(β) stretching mode of T4 is observed at

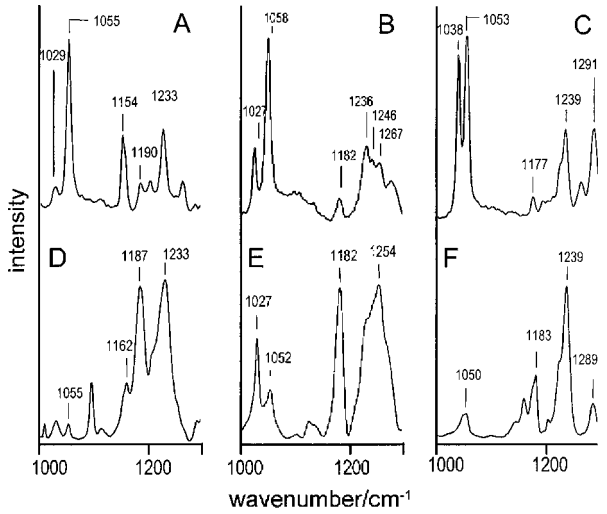

Figure 4. Raman spectra of (A) T4, (B) T3 and (C) T2 in the region between 1000 and 1300 cm^{-1}. Infrared spectra of (D) T4, (E) T3 and (F) T2 in the region between 1000 and 1300 cm^{-1}.

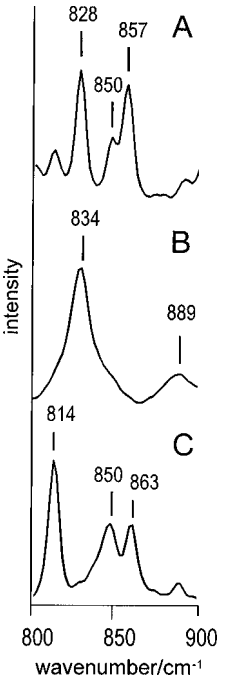

Figure 5. Raman spectra of (A) T4, (B) T3 and (C) T2 in the region between 800 and 900 cm^{-1}.

ca 1180 cm^{-1}, which is very similar to those observed for T2 and T3.

The C–N stretching coordinate contributes to a mode which is calculated at ca 1090 cm^{-1} with medium Raman and weak IR intensity. Owing to the intensity pattern, this mode is assigned to the experimental bands at 1055, 1058 and 1053 cm^{-1} of T2, T3 and T4, respectively. The ring mode $\alpha(9)$, for which a strong Raman intensity is predicted, appears with weak and medium intensity at 1029 and 1027 cm^{-1} in the experimental Raman spectra of T2 and T3, respectively. The corresponding strong band at 1038 cm^{-1} in the Raman spectrum of T4 may in addition include the $\beta(9)$ mode for which, owing to same iodine substitution, the wavenumber is predicted to be similar to that of the $\alpha(9)$ mode.

Tyrosine and related molecules display a doublet at ca 850–830 cm^{-1} in the Raman spectrum, which is due to Fermi resonance between the ring-breathing mode and the overtone of an out-of-plane ring bending vibration.[23] Since this doublet has been observed for a large number of *para*-substituted benzenes with C_{2v} local symmetry, we carefully analysed this region for the thyroid hormones, especially T2 and T4.

In the Raman spectrum of T2, two signals of equal medium intensity are observed at 863 and 850 cm^{-1} (Fig. 5). The only fundamental mode that could plausibly be ascribed to one of the observed signals is the ring-breathing $\beta(12)$ mode, calculated at 833 cm^{-1}. The second mode in this region, for which a considerable Raman intensity and the same wavenumber (801 cm^{-1}) for all three hormones is predicted, is an in-plane deformation involving the both aromatic rings. This mode is assigned to the intense Raman band at 814 cm^{-1} on comparison with the calculated wavenumber and intensity. On the basis of this assignment, there is no other fundamental mode that can be attributed to the medium-intensity band at 863 cm^{-1}. Hence we attribute the 863 cm^{-1} band to an overtone that, in analogy with tyrosine, gains intensity via Fermi resonance with the mode $\beta(12)$. The most likely candidate is the overtone of $\tau\beta$, calculated at 420 cm^{-1}, owing to the good agreement between the predicted and experimentally observed wavenumber (2×420 cm^{-1} vs 863 cm^{-1}) and the localization $\tau\beta$ and $\beta(12)$ in the same ring. Unfortunately, only a very weak Raman intensity is predicted for the fundamental $\tau\beta$, which is in fact not observed in the experimental Raman spectrum.

The same considerations hold for the assignment of the 850 and 857 cm^{-1} bands of T4, which also have been attributed to the fundamental $\beta(12)$ and the overtone of $\tau\beta$, respectively.[9] In T4, this out-of-plane deformation of the phenolic ring is calculated at 492 cm^{-1}, and is assigned to the 430 cm^{-1} IR band. This relatively large difference between the calculated and the observed wavenumbers can be rationalized in terms of the substantial deviation between the calculated and experimental dihedral angles of the α-ring/β-ring linkage (Table 1), which may have a specifically strong impact on the out-of-plane modes.

It may be that these deviations are less pronounced for T2 in view of the much better agreement of the overtone $2\tau\beta$ with the observed wavenumber. Unfortunately, no experimental data for the structure of T2 are available and the fundamental $\tau\beta$ is not detectable in the experimental Raman spectrum.

In tyrosine and related compounds, the intensity distribution between the fundamental and the overtone of the Fermi doublet can be used to draw qualitative conclusions about

JRS

the strength of hydrogen bond interactions of the phenolic hydroxyl group. It has been shown that for weakly hydrogen bonded tyrosine derivatives, the fundamental exhibits a higher Raman intensity,[23] as is also observed for T2. In view of the similar band positions, one may conclude that this empirical relationship may also hold for T4 despite the substitution of two hydrogens by iodines. Then the intensity decrease of the fundamental would indicate stronger hydrogen bond interactions in T4 than T2, presumably brought about by the iodine substituents of the phenol ring.

The Raman spectrum of T3 displays a different picture inasmuch as the doublet is missing and the only band in this region is the broad and asymmetric peak centred at 834 cm^{-1}, which may originate from the α/β ring deformation and the modes $\beta(12)$ and $\beta(14a)/\beta(14b)$. In contrast to T3, ring β of T2 and T4 exhibits a symmetric substitution pattern which appears to be a prerequisite for the Fermi resonance enhancement of $2\tau\beta$.

The strongest bands in the Raman spectra of iodothyronines are found between 150 and 250 cm^{-1} and are attributed to the C–I stretchings (Fig. 6). The vibrational band pattern in this region is different for the three hormones, reflecting the different numbers of iodine substituents. On the basis of the calculated wavenumbers, a consistent assignment is achieved even though there are discrepancies between the experimental and the calculated Raman intensities which are likely to originate from the intrinsic deficiencies of the B3LYP/SDD level of theory for treating iodine atoms.

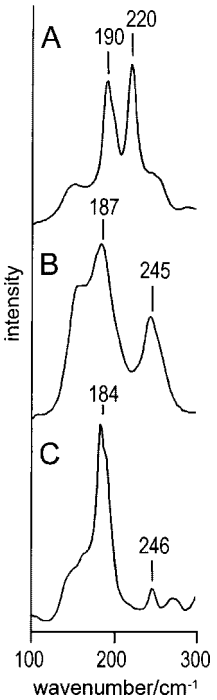

Figure 6. Raman spectra of (A) T4, (B) T3 and (C) T2 in the region between 100 and 300 cm^{-1}.

The two C–I stretching modes in T2 are assigned to the 246 and 184 cm^{-1} bands that exhibit a weak and a very strong Raman intensity, respectively. Similar wavenumbers are calculated and observed for these two vibrations in T3. The stretching mode that originates the additional C—I bond in the phenolic ring is not observed owing to the overlap with the antisymmetric C–I(α) mode. The Raman spectrum of T4 shows two very strong peaks at 220 and 190 cm^{-1}. According to the calculated wavenumbers and by comparison with T2 and T3, they are attributed to the symmetric C–I(β) and C–I(α) stretching modes, respectively. The antisymmetric modes appear as a shoulder at ca 245 cm^{-1}.

CONCLUSION

On the basis of IR and Raman spectroscopy and supported by DFT calculations, a consistent vibrational analysis of iodothyronines is possible which constitutes the basis for extracting structural data from the spectra of hormone/lipid complexes. The different effects that thyroxine and its analogues 3,5,3′-triiodothyronine and 3,5-diiodothyronine produce on the physicochemical properties of membranes are most likely due to the specific conformations that can be adopted after inserting into the lipid bilayer. This conformational adaptation depends on rotational energies, particularly of the ring-α/ring-β linkage, and on steric requirements. Both factors are different in T2, T3 and T4. On the basis of the present study, it is now possible to identify modes including those internal coordinates that are expected sensitively to reflect different conformations of the hormones upon binding to membranes. These are in particular the coordinates of the ether bridge and the C–I stretchings. Future vibrational spectroscopic studies on the interaction of T2, T3 and T4 with phospholipid bilayers may provide further information on the conformations of the various iodothyronines, which is a prerequisite for understanding their functioning on a molecular basis.

Acknowledgements

R.M.S.Á. and R.N.F. thank the Universidad Nacional de Tucumán and CONICET, Argentina, and DAAD for financial support.

REFERENCES

1. Hennemann G, Docter R, Friesema EC, de Jong M, Krenning EP, Visser TJ. *Endocr. Rev.* 2001; **22**: 451.
2. Chehin RN, Isse BG, Rintoul MR, Farias RN. *J. Membr. Biol.* 1999; **167**: 251.
3. Farías RN, Chehin RN, Rintoul MR, Morero RD. *J. Membr. Biol.* 1995; **143**: 135.
4. Chehin RN, Rintoul MR, Morero RD, Farías RN. *J. Membr. Biol.* 1995; **147**: 217.
5. Hillier AP. *J Physiol.* 1970; **211**: 585.
6. Hulbert AJ. *Biol. Rev.* 2000; **75**: 519.
7. Tsybulskaya MV, Antonenko NYu, Tropsha AE, Yaguzhinsky LS. *Biofizika* 1984; **29**: 801.
8. Isse BG, Fidelio G, Farias RN. *J. Membr. Biol.* 2003; **191**: 209.

9. Álvarez RMS, Della Védova CO, Mack H-G, Farías RN, Hildebrandt P. *Eur. Biophys. J.* 2002; **31**: 448.
10. Camerman A, Camerman N. *Acta Crystallogr., Sect. A* 1974; **30**: 1832.
11. Matysik J, Hildebrandt P, Schalamann W, Braslavsky SE, Schaffner K. *Biochemistry* 1995; **34**: 10 497.
12. Frisch MJ, Trucks GW, Schlegel HB, Scuseria GE, Robb MA, Cheeseman JR, Zakrzewski VG, Montgomery JA, Stratman RE, Burant JC, Dapprich S, Millam JM, Daniels AD, Kudin KN, Strain MC, Farkas O, Tomasi J, Barone V, Coss Mi, Cammi R, Menucci B, Pomelli C, Adamo C, Clifford S, Ochterski J, Petersson GA, Ayala PY, Cui Q, Morokuma K, Malick DK, Rabuck AD, Raghavachari K, Foresman JB, Cioslovski J, Ortiz JV, Stefanov BB, Liu G, Liashenko A, Piskorz P, Komaromi I, Gomperts R, Martin RL, Fox DJ, Keith T, Al-Laham MA, Peng CY, Nanayakkara A, Gonzales C, Challacombe M, Gill PMW, Johnson B, Chen W, Wong MW, Andres JL, Head-Gordon M, Replogle ES, Pople JA. *Gaussian 98 (Revision A.7)*. Gaussian: Pittsburgh, PA, 1998.
13. Cody V, Duax WL, Norton DA. *Acta Crystallogr., Sect. B* 1972; **28**: 2244.
14. Cody V. *J. Am. Chem. Soc.* 1974; **96**: 6720.
15. Fawcett JK, Camerman N, Camerman A. *J. Am. Chem. Soc.* 1976; **98**: 587.
16. Cody V. *Endocr. Rev.* 1980; **1**: 140.
17. Qin Y, Wheeler A. *J. Am. Chem. Soc.* 1995; **117**: 6083.
18. Frey MN, Koetzle TF, Lehmann MS, Hamilton WC. *J. Chem. Phys.* 1973; **58**: 2547.
19. Magdó I, Nemeth K, Mark F, Hildebrandt P, Schaffner K. *Phys. Chem. A*, 1999; **103**: 289.
20. Pulay P, Fogarasi G, Pongor G, Boggs JE, Vargha A. *J. Am. Chem. Soc.* 1983; **105**: 7037.
21. Harada I, Takeuchi H. In *Spectroscopy of Biological Systems*, vol. 13, Clark RJH, Hester RE (eds). Wiley: New York, 1986; 113.
22. Lai G-S, Korotowsky W, Chien H-N, Cheng S-Y. *Biochem. Biophys. Res. Commun.* 1985; **131**: 408.
23. Siamwiza MN, Lord RC, Chen MC, Takamatsu T, Harada I, Matsuura H, Shimanouchi T. *Biochemistry* 1975; **14**: 4870.